AD NUMBER

AD880431

NEW LIMITATION CHANGE

TO

Approved for public release, distribution unlimited

FROM

Distribution authorized to U.S. Gov't. agencies and their contractors; Critical Technology; JAN 1971. Other requests shall be referred to Ballistic Research Labs., Aberdeen Proving Ground, MD.

AUTHORITY

USAARADCOM ltr, 24 Feb 1981

BRL

REPORT NO. 1524

SENSITIVITY STUDY OF RIFLE GAS SYSTEMS

by

Nathan Gerber

January 1971

U.S. ARMY ABERDEEN RESEARCH AND DEVELOPMENT CENTER
BALLISTIC RESEARCH LABORATORIES
ABERDEEN PROVING GROUND, MARYLAND

Destroy this report when it is no longer needed.
Do not return it to the originator.

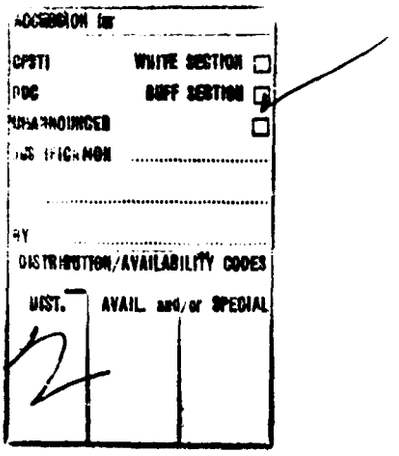

The findings in this report are not to be construed as an official Department of the Army position, unless so designated by other authorized documents.

B A L L I S T I C R E S E A R C H L A B O R A T O R I E S

REPORT No. 1524

JANUARY 1971

SENSITIVITY STUDY OF RIFLE GAS SYSTEMS

Nathan Gerber

Exterior Ballistics Laboratory

RDT&E Project No. 1T061102A33D

A B E R D E E N P R O V I N G G R O U N D, M A R Y L A N D

B A L L I S T I C R E S E A R C H L A B O R A T O R I E S

REPORT NO. 1524

NGerber/smo
Aberdeen Proving Ground, Md.
January 1971

SENSITIVITY STUDY OF RIFLE GAS SYSTEMS

ABSTRACT

Results of a sensitivity study of the M-16 rifle gas system are presented; this study is based on a simulation of rifle gas system operation developed in the BRL. The calculations indicate that thermodynamic variables in the bolt carrier cavity are only weakly sensitive to variations in the following parameters: i) pressure and temperature in the gun barrel when the bullet passes the port, ii) friction in the duct flow, and iii) frictional resistance to motion of the bolt carrier. The computational results are sensitive, however, to the chosen origin of time on the oscillogram showing barrel pressure at the port station.

Graphs are presented for a typical round illustrating pressure, temperature, density, and piston motion histories for M-16 and AR-18 rifle gas systems.

Preceding page blank

TABLE OF CONTENTS

 Preceding page blank

LIST OF ILLUSTRATIONS

LIST OF SYMBOLS

$\bar{c}_p$	specific heat at constant pressure [Nm/(kg deg K)]
$\bar{c}_v$	specific heat at constant volume [Nm/(kg deg K)]
$\bar{e}$	($\equiv \bar{c}_v \bar{\theta}$) internal energy per unit mass [Nm/kg]
f	friction factor
$\bar{h}$	enthalpy per unit mass [Nm/kg]
$\bar{k}$	thermal conductivity of powder gas [(kg m)/(sec^3 $^\circ$K)]
$\bar{\ell}$	length of gas tube [m]
$\bar{m}$	$\equiv \bar{A}_e \bar{\rho}_e \bar{u}_e$ [kg/sec]
$\bar{p}$	pressure [kg/(m sec^2)]
$\bar{r}_v$	radius of vent cross-section [m]
$\bar{t}$	time [sec]
$\bar{u}$	gas velocity [m/sec]
$\bar{v}_B$	velocity of bolt carrier with respect to bolt [m/sec]
$\bar{x}$	distance from port in gas tube [m]
$\bar{x}_B$	displacement of bolt carrier [m]
$\bar{x}_{BE}$	maximum displacement of bolt carrier [m]
$\bar{x}_{Bv}$	location of center of vent [m]
$\bar{A}_c$, $\bar{A}_e$, $\bar{A}_v$	cross-sectional areas of cavity, cavity entrance, and vent, respectively [m^2]
$\bar{A}_{min}$, $\bar{A}_p$	areas at throat and exit of port, respectively [m^2]
$\bar{D}$ ($=[4\bar{A}_e/\pi]^{1/2}$)	cross-sectional diameter of gas tube [m]
K_F, K_B	resistance coefficients due to friction and bends
$\bar{M}_B$	mass of bolt carrier [kg]
$\bar{R}_{gas}$	effective gas constant for powder gas [Nm/(kg deg K)]

$\bar{V}_c$	volume of cavity [m^3]
$\bar{V}_{ci}$	$= \bar{V}_c$ $(\bar{t} = 0)$
α_e	contraction coefficient--backward flow from cavity into duct
α_p	contraction coefficient--backward flow from duct into port
α_g	contraction coefficient--forward flow from gun barrel into port
$\Delta\bar{t}_d$	time interval between initial rise of barrel pressure oscillogram and $\bar{t} = 0$ axis
γ	effective ratio of specific heats of gas
$\hat{\gamma}$	exponent in $\bar{p}_g$, $\bar{\theta}_g$ relation
$\hat{\gamma}$	ratio of specific heats for gas initially present in gas tube ($\approx$ 1.4 for air)
$\bar{\epsilon}/\bar{D}$	relative roughness of duct
$\bar{\theta}$	temperature [deg K]
$\bar{\mu}$	viscosity coefficient of powder gas [kg/(m sec)]
$\bar{\rho}$	density [kg/m^3]
$\bar{\phi}$	resistance forces on piston [N]

Subscripts

c	bolt chamber
e	entrance to cavity
g	gun barrel at port station
i	initial value $(\bar{t} = 0)$
E	end of piston motion

BLANK PAGE

I. INTRODUCTION

It is desirable to simulate the operation of the gas system which extracts a spent cartridge and positions the next round in the chamber of an automatic gas-operated rifle. The operation cycle is a rather complicated gasdynamic process and must necessarily be described with a considerably simplified model.

The model developed in Reference 1* has proven to be reasonably accurate in predicting pressure history for the bolt cavity of the M-16 rifle. This model is applicable to the firing of all rifles during the initial interval before moving parts interact in the reloading mechanism. This interval covers a small portion (~1/20th) of the total operation time, but during this period the pressure and temperature attain their peaks and the system receives all its momentum from the powder gas.

The above model forms the basis for this report. In particular, we shall study the sensitivity of the gas system to variations in input data. Since it is not possible to survey in detail the many factors which affect the performance, attention will be concentrated on several of the more notable effects caused either by change of conditions inside of the gun (e.g., friction in gas duct, change of ammunition) or uncertainties resulting from measurements (e.g., zero time and peak pressure at gas duct entrance).

The basic analysis, assumptions, and approximations are described thoroughly in Reference 1 and will not be repeated in detail here. A brief outline of the model is given in Section II. Results of computations and measurements for the M-16 rifle, including data for the sensitivity study, are presented to illustrate general behavior of gas systems. Finally, data are presented for the AR-18 rifle, and some comparisons with M-16 results are made.

---

*Current computations employ the "area discontinuity" treatment of the gun tube port, treated in the ADDENDUM of Reference 1. References are listed on page 37.

II. THEORETICAL MODEL OF GAS SYSTEM

For the early stage of the operation cycle, rifle gas systems are essentially equivalent to the system represented by the idealized geometry shown in Figure 1.* Hot, high-pressure powder gases are extracted from the rifle barrel and fed through a duct into a chamber, where the gases expand, thereby accelerating a piston. After the piston has traveled a certain distance, vent holes are laid free and the gas in the chamber expands to atmosphere. The pressure, temperature and density of the powder gas in the barrel -- $\bar{p}_g(\bar{t})$, $\bar{\theta}_g(\bar{t})$, $\bar{\rho}_g(\bar{t})$ -- are known, and constitute the input to the problem.

The quantities to be determined are the flow variables in the chamber and the motion of the piston. The equations to be solved are:[1]

$$\bar{A}_e \bar{\rho}_e \bar{u}_e = (\bar{V}_{ci} + \bar{A}_c \bar{x}_B)(d\bar{\rho}/d\bar{t}) + \bar{A}_c \bar{\rho}_c \bar{v}_B + \text{venting term} \qquad (1)$$

$$\bar{m}\,\bar{h}_{e\ tot} = d/d\bar{t}\,[\bar{\rho}_c \bar{e}_c \bar{V}_c + 1/2\,\bar{\rho}_c \bar{v}_B^{\,2}\,\bar{V}_c + \bar{A}_c \int_0^{\bar{t}} \bar{p}_c \bar{v}_B d\bar{t}] + \text{venting terms} \qquad (2)$$

$$d\bar{v}_B/d\bar{t} = \bar{p}_c \bar{A}_c \bar{M}_B^{-1} + \bar{\Phi}\,\bar{M}_B^{-1} \qquad (3)$$

$$d\bar{x}_B/d\bar{t} = \bar{v}_B \qquad (4)$$

$$\bar{p} = \bar{R}_{gas}\,\bar{\rho}\,\bar{\theta} \qquad (5)$$

where $\bar{m} = \bar{A}_e \bar{\rho}_e \bar{u}_e$ $\qquad$ $\bar{h}_{e\ tot} = \bar{p}_e/\bar{\rho}_e + \bar{e}_e + \bar{u}_e^{\,2}/2$

$\bar{e} = \bar{c}_v\,\bar{\theta}$ $\qquad$ $\bar{V}_c = \bar{V}_{ci} + \bar{A}_c \bar{x}_B$

This report uses the notation of Reference 1; definitions of symbols are found in LIST OF SYMBOLS.

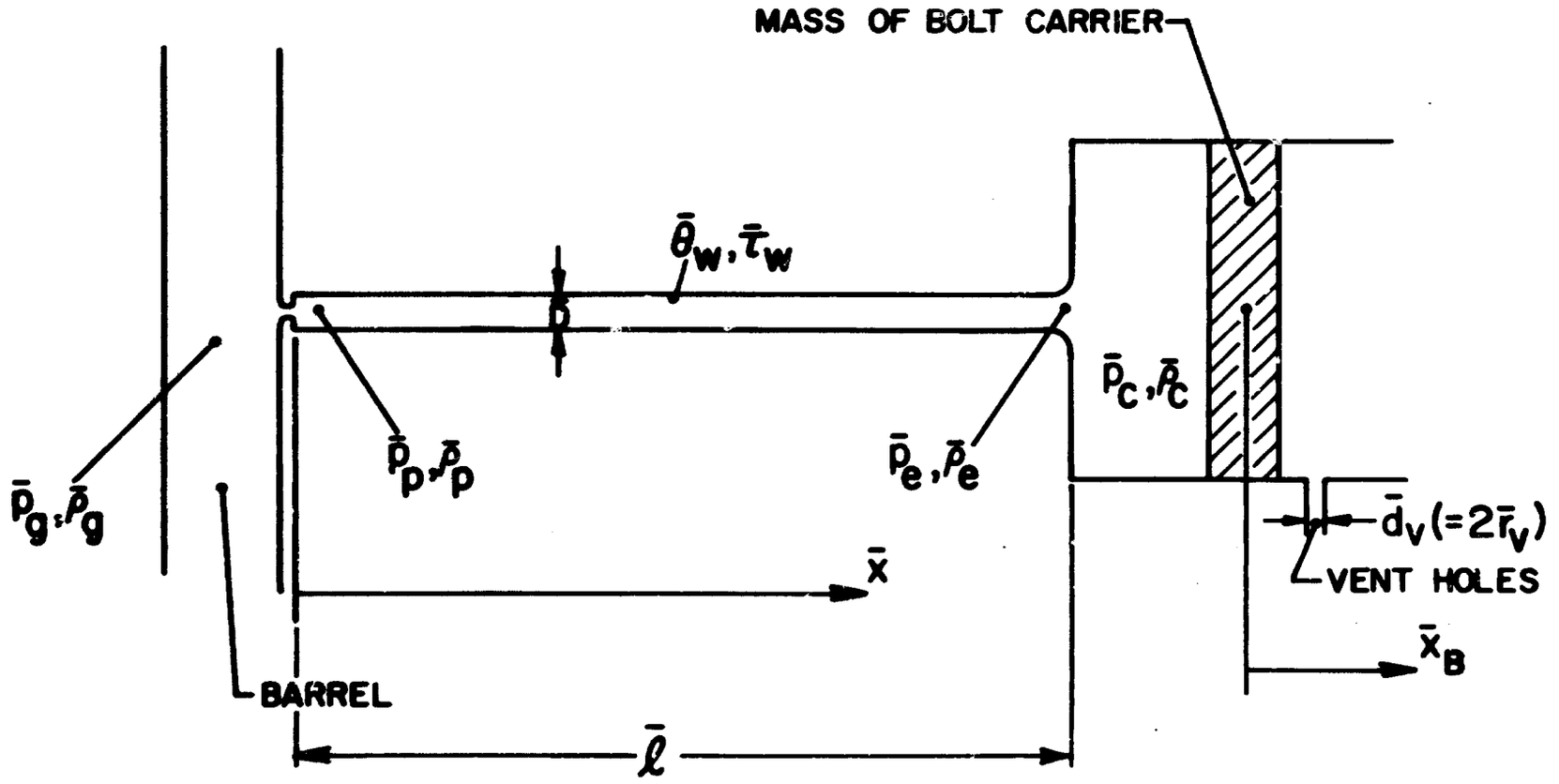

Figure 1. Idealized Geometry for Rifle Gas System

For computations thus far performed, $\bar{\theta}_c = 300^{\circ}K$, $\bar{p}_c = 1$ atm, $\bar{x}_B = 0$, $\bar{v}_B = 0$ at $\bar{t} = 0$.

The quantities at the entrance to the chamber (e) remain to be determined. This determination, however, entails the solution of partial differential equations for the unsteady viscous heat-conducting flow through the duct, with initial and boundary conditions that require matching this flow on the one side to conditions in the barrel (via the port), and on the other side to conditions in the chamber. The procedures for obtaining solution are described in Reference 1.

Of prime significance is the friction factor f occuring in the momentum equation (also, by Reynolds analogy, in the energy equation):

$$\partial\bar{u}/\partial\bar{t} + \bar{u}\,\partial\bar{u}/\partial\bar{x} + (1/\bar{\rho})\,\partial\bar{p}/\partial\bar{x} + (2\,f\,\bar{u}^{2}/\bar{D}) = 0$$

It includes losses due to bends as well as to friction in the duct and is given by

$$f = [\bar{D}/(4\bar{L})]\,(K_F + K_B) \qquad (C)$$

where K_F and K_B are values taken from handbooks.[2] Since the value of f is an estimate at best, it is taken to be a constant, adjusted within limits to give best agreement with experiment.

The analysis assumes an instantaneous pressure rise in the barrel at the port and predicts the delay between this instant and the beginning of pressure rise in the chamber.

III. STUDY OF M-16 GAS SYSTEM

A. Introductory Remarks.

Since all rifle gas systems can be treated as the basic configuration of Figure 1 for early times, it is expected that some general information could be extracted from the study of a particular system—in this case, that of the M-16 rifle, shown in Figure 2. The bolt carrier

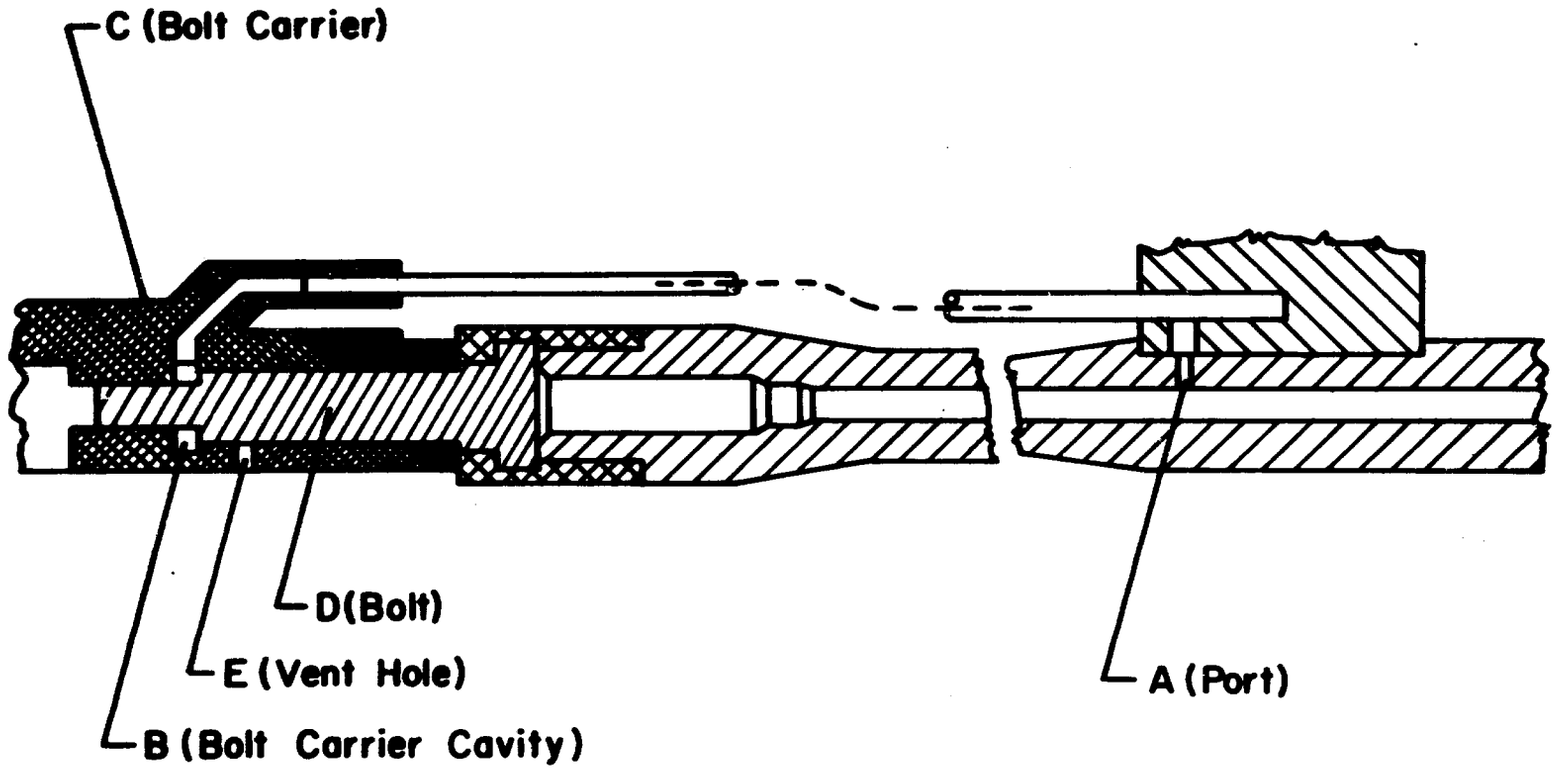

Figure 2. Design Sketch of M-16 Rifle

assumes the role of the piston here, and the annular bolt carrier cavity is the chamber of Figure 1. Properties of the powder gas, dimensions of the gas system, and loss coefficients are given in APPENDIX A. Input data for the numerical study are drawn mainly from two rounds fired with different ammunition, which will be referred to as "lot #1" and "lot #2".

B. Input Data

The accuracy of the results of the computation depends on the accuracy with which the input pressure is measured. In the experiments static pressures were recorded on calibrated oscillograms (as traced in Figure 3). Unfortunately, because of certain experimental factors, e.g., electronic circuit delays, it has been impossible so far to determine accurately the initial pressure behavior from Figure 3. The dip in pressure near the peak, and possibly the peak dip, was caused by a change in ground potential of electrical equipment. It is necessary to smooth this dip and other spurious signals.

Computations shown in Figure 4a indicate that changing the peak pressure by 13% has little effect on the cavity pressure.

Reference time ($\bar{t}$=0) in the computation is taken as the time at which the pressure pulse appears at the port. The computation assumes that the pressure rises suddenly to $\bar{p}_{max}$ at the instant the bullet passes the port. However, this time is not well defined in the experiment. Between rise of pressure and maximum of the pressure there is a time interval of about 0.1×10^{-3} sec. The origin is thus uncertain by $|0.05 \times 10^{-3}|$ sec. Experimentally this uncertainty may be caused by finite response times, but also it is noted that the shock wave which precedes the bullet and gas blown by the bullet cause an earlier rise in pressure.

To study the effect of location of reference time on cavity pressure, the origin of time was shifted in the computations by various values $\Delta\bar{t}_d$ from the instant of pressure rise on the port pressure oscillogram. Results are shown in Figure 4b. Best agreement occurs for

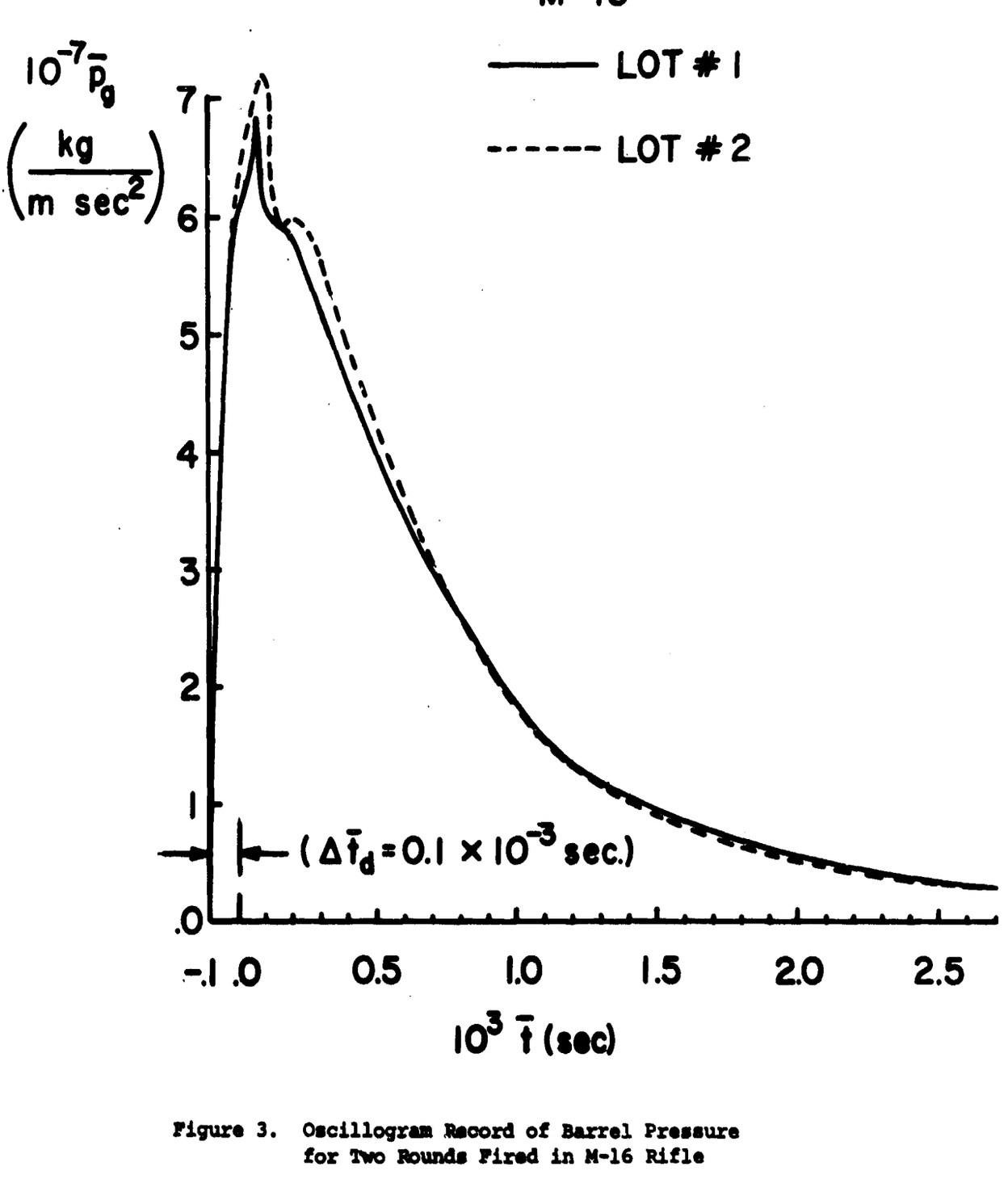

Figure 3. Oscillogram Record of Barrel Pressure for Two Rounds Fired in M-16 Rifle

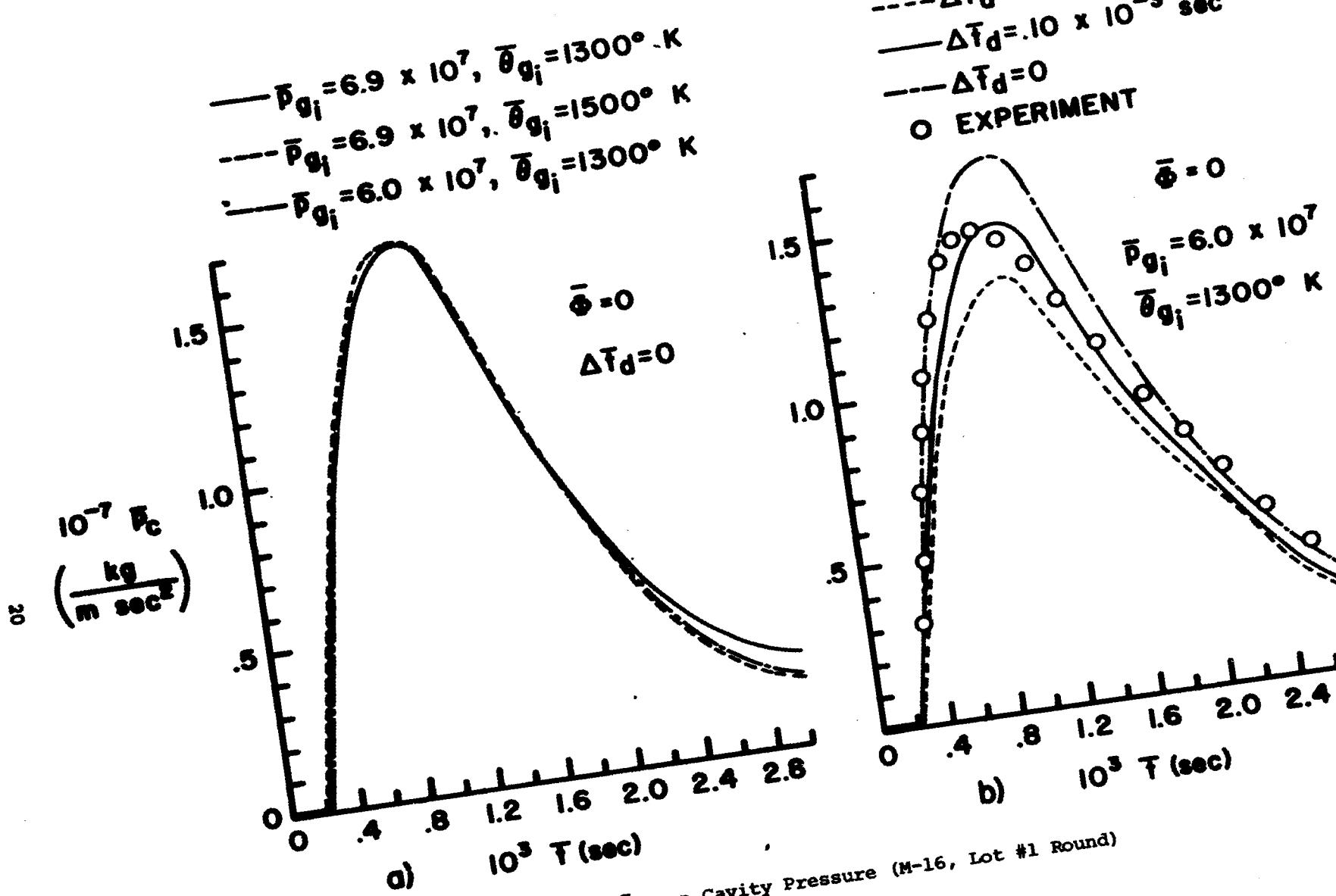

Figure 4. Effect of $\bar{P}_{g_i}$, $\bar{\theta}_{g_i}$, $\bar{\Delta t}_d$ on Cavity Pressure (M-16, Lot #1 Round)

$\Delta\bar{t}_d = 0.1 \times 10^{-3}$ sec. When this value is applied as a correction to the measured delay between the rise times of port pressure and cavity pressure ($\simeq 0.3 \times 10^{-3}$ sec.), a delay of 0.2×10^{-3} sec. results. As stated in Section II, the gas system model predicts the delay time. In the present instance it predicts a delay of 0.2×10^{-3} sec., in agreement with the value determined above.

The influence of difference in ammunition is indicated in Figure 3 for two rounds. The greatest difference in pressure appears in the first half-millisecond of the cycle; the ultimate effect on cavity pressure will be shown in Figure 5.

The temperature at the port is also required input for the calculation, and is computed according to

$$\bar{\theta}(\bar{t})/\bar{\theta}(0) = [\bar{p}(\bar{t})/\bar{p}(0)]^{(\tilde{\gamma} - 1)/\tilde{\gamma}}$$

The initial temperature $\bar{\theta}_g(0)$ was not accurately determined for the rounds fired, and an estimate was required. Fortunately, however, calculations shown in Figure 4a indicate that within limits (1300°-1500°K in this case) an exact knowledge of the temperature is not extremely crucial.

C. Cavity Pressure

1. Comparison with Experiment. Pressure is the variable of prime interest here, and it will be examined in most detail. Pressure histories computed for the bolt chamber are shown in Figure 5. Agreement with experiment is quite good. Maximum pressure is reached in the chamber about 1×10^{-3} sec. after the bullet has passed the port station in the barrel.

2. Effect of Ammunition. The two input curves in Figure 3, representing the effect of change of ammunition, yield the two theoretical cavity pressure-time curves in Figure 5. The difference in peak values is about fifteen per cent.

3. Effect of Friction in Duct. The frictional resistance to flow in the duct causes pressure losses which reduce the pressure in the bolt chamber. This resistance is incorporated into the model by means of the

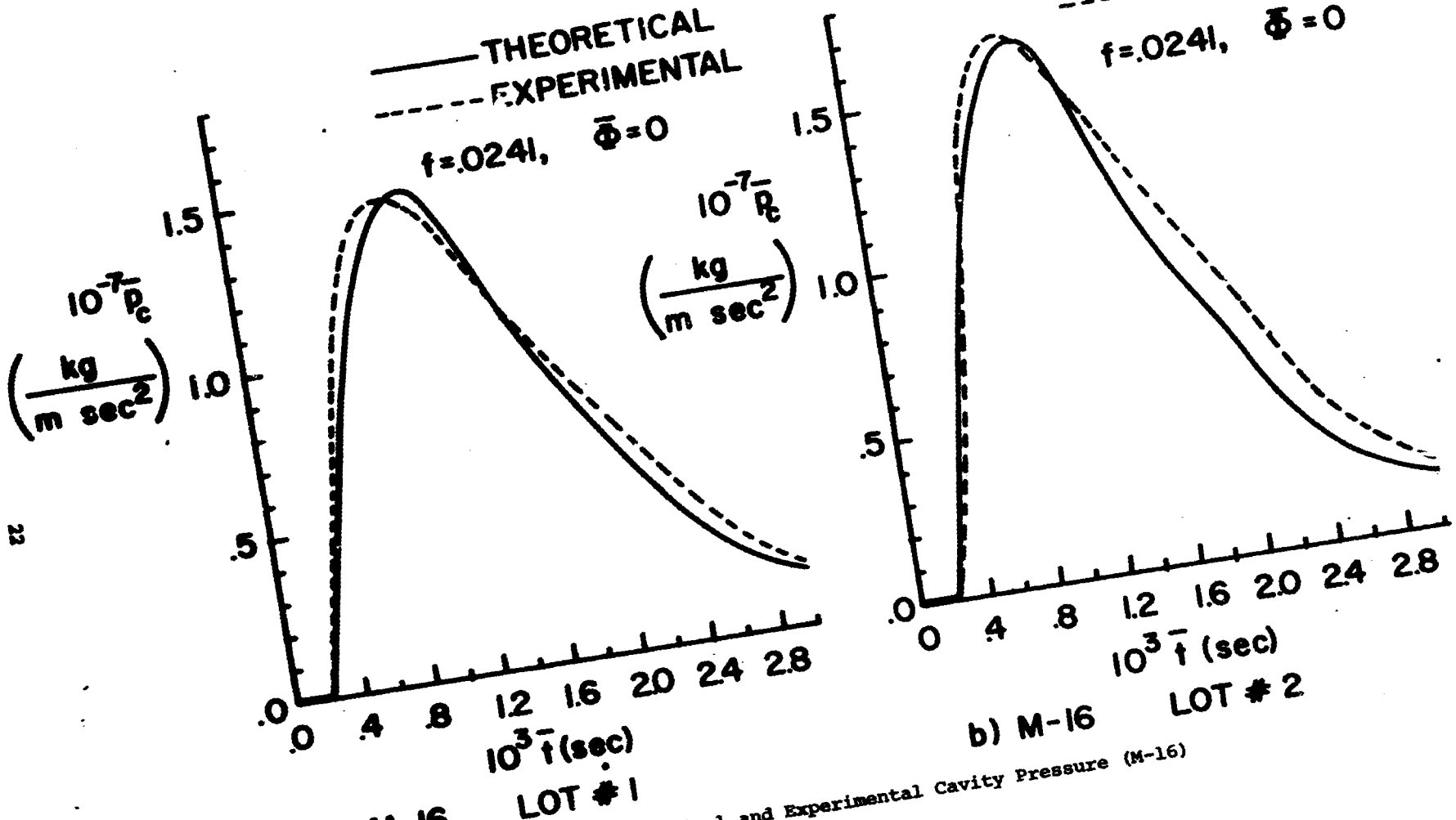

Figure 5. Comparison of Theoretical and Experimental Cavity Pressure (M-16)

"friction factor" f. Powder gas particles accumulated from successive firings adhere to the wall of the duct and thereby produce progressive change in the friction factor. The quantity f is difficult to measure accurately and (as stated in Section II) it must be eventually estimated even after an appropriate value range is determined with the aid of handbook data.

In Figure 6 are shown cavity pressure histories for three values of f(=.0210, .0241, .0270, where .0241 is the nominal handbook value).* The conclusion is that the pressure is not a sensitive function of f in the range which yields optimum agreement with measurements. On the scale to which the curves are plotted the only notable differences can be found near the peak, where a twenty-five per cent variation in f produces only a seven per cent variation in maximum pressure. All these curves fall below experimental pressure values on the right hand side.

The f=0 curve (drawn to half scale in Figure 6) demonstrates the decided effect that the presence of friction and heat conduction has on the pressure in the chamber. Without inclusion of friction the pressure rises to a maximum about two and a half times that of the measured peak in about two-thirds of the time taken to attain the latter, and then drops at a rate several times that of the measured pressure. The f = 0 curve can be viewed as the limiting case for diminishing friction in the duct flow; it is then seen that the sensitivity of the pressure to changes in f will increase as f decreases.

4. Frictional Resistance to Piston Motion. Inclusion of forces resistant to the motion of the bolt carrier, $\bar{\Phi}$ in Eq. (3), should improve agreement between theory and experiment. An estimate of the magnitude of the forces involved can be gained by a knowledge of the discrepancies, as in Figure 6. However, the friction force law is not presently known in this situation.

A simplified friction law was assumed and two cases computed with it: namely, that the piston does not move until the cavity pressure reaches a preassigned value $\bar{p}_z$, then it moves against a force

---

*Because the friction factor depends on the particular gas system, through Eq. (6), the value of f can vary widely from one gun system to another.

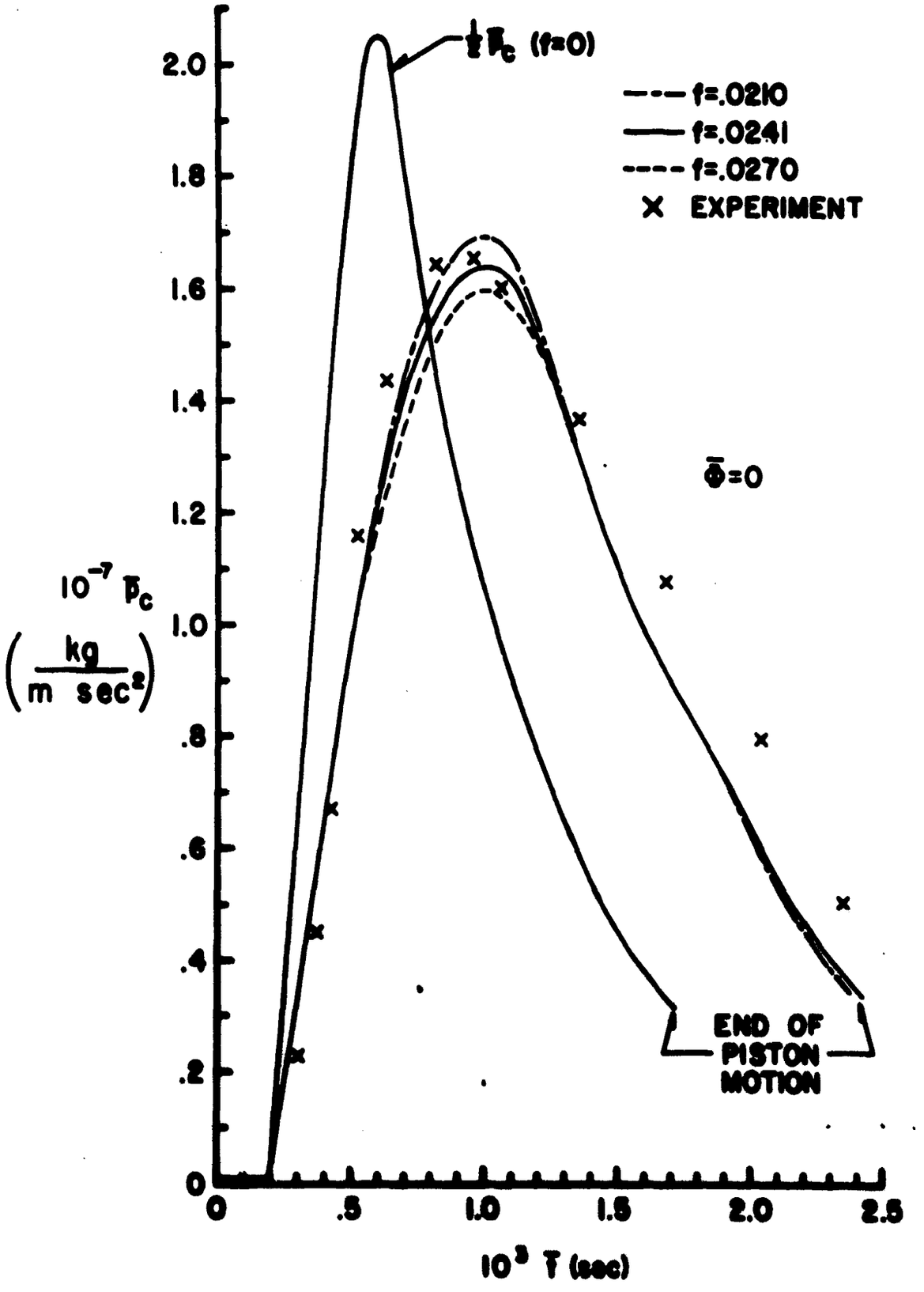

Figure 6. Effect of Friction Factor f on Cavity Pressure (M-16, Lot #2 Round)

$\bar{\Phi} = -\lambda \bar{p}_c \bar{A}_c$, where $0 < \lambda = \text{const.} < 1$. Results shown in Figure 7 indicate that this model does not uniformly improve agreement with experiment; there is a tendency to produce peak pressures too high in the process of closing the gaps on the sides of the curves. More study will be required on this subject.

5. Effect of Jamming. To determine the effect of gas system jamming on cavity pressure, a computation was performed in which $\bar{v}_B$ was set equal to zero for $t \geq 2.05 \times 10^{-3}$ sec. The result is shown in Figure 8 for a particular round. A pressure rise occurs immediately after the piston stops, then the pressure decreases at a slower rate than for the unimpeded piston. Qualitatively this behavior has been confirmed by experiments.

D. Cavity Temperature and Density

Temperature and density histories in the cavity are plotted in Figures 9 and 10. It is seen that the temperature reaches peak value very rapidly; the cooling which then follows is due to the expansion of the gases in the expanding cavity as well as to the decrease of $\bar{\theta}_g$ with time. This cooling brings the temperature down to the range of its initial value (in this case, below it) within the first 2.4×10^{-3} sec.

The density attains its maximum at approximately 1×10^{-3} sec., and at 2.4×10^{-3} sec. it is still about twenty times its initial value.

The rates of fall of temperature and density are increased slightly when the vent is uncovered.

A survey of the calculations shows that temperature and density are generally affected less than pressure by the variations of the parameters discussed above in Subsection C. The limiting case of zero heat conduction and friction ($f = 0$) again has a marked effect; the peak temperature increases by a factor of four, and the peak density is cut by about one-half of its value.

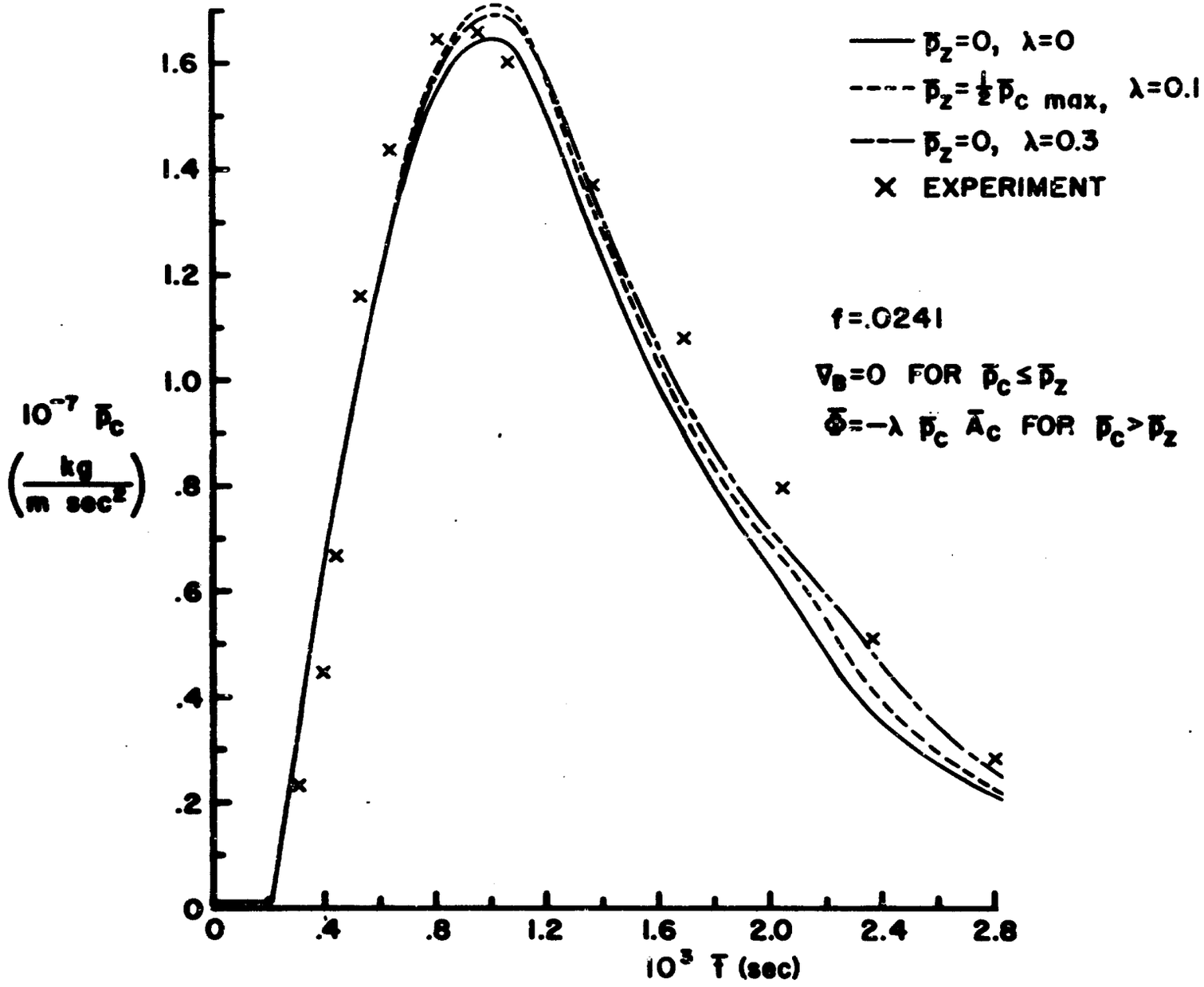

Figure 7. Effect on Cavity Pressure of Frictional Resistance to Piston Motion (M-16, Lot #2 Round)

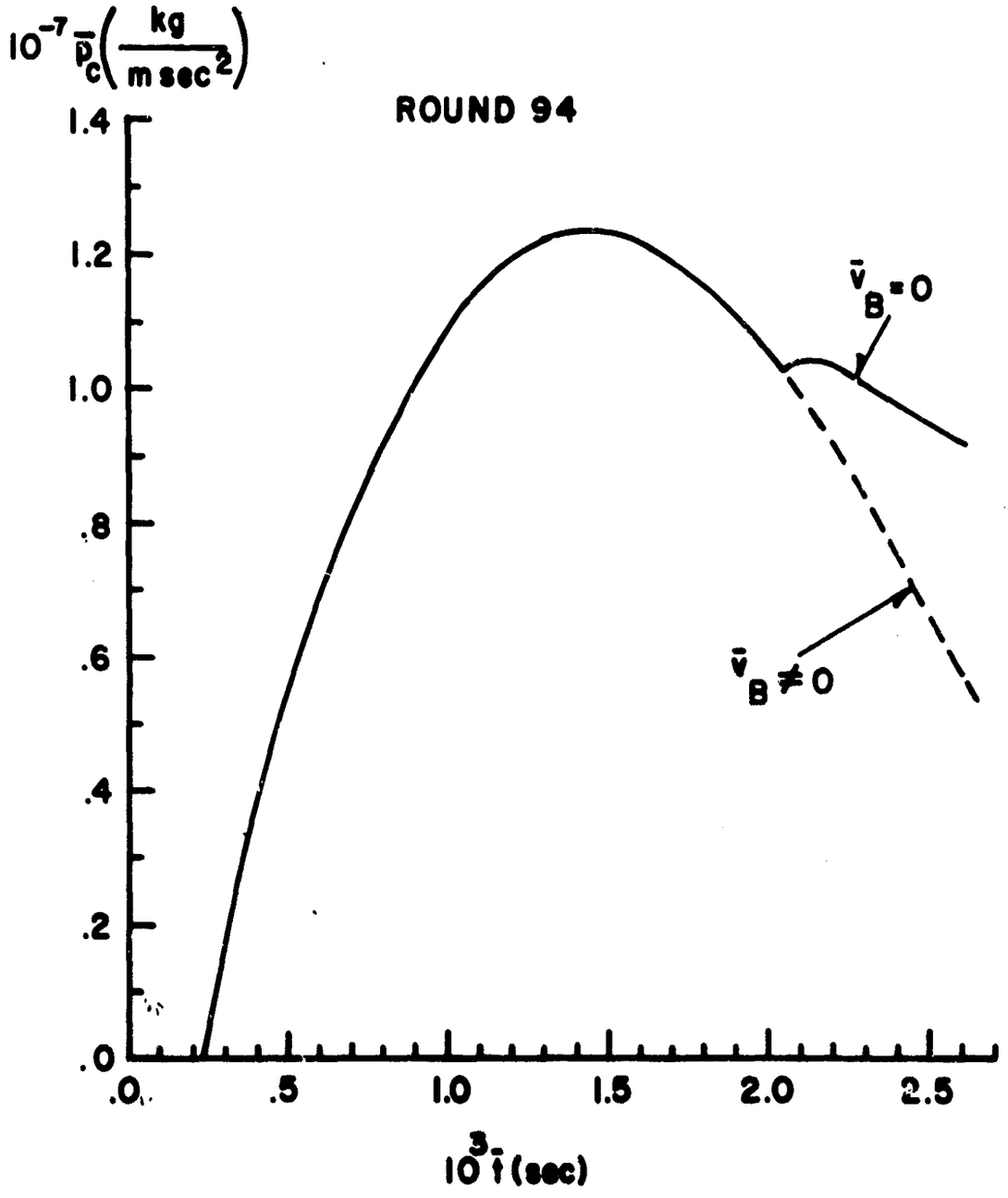

Figure 8. Effect of Jamming on Cavity Pressure (M-16)

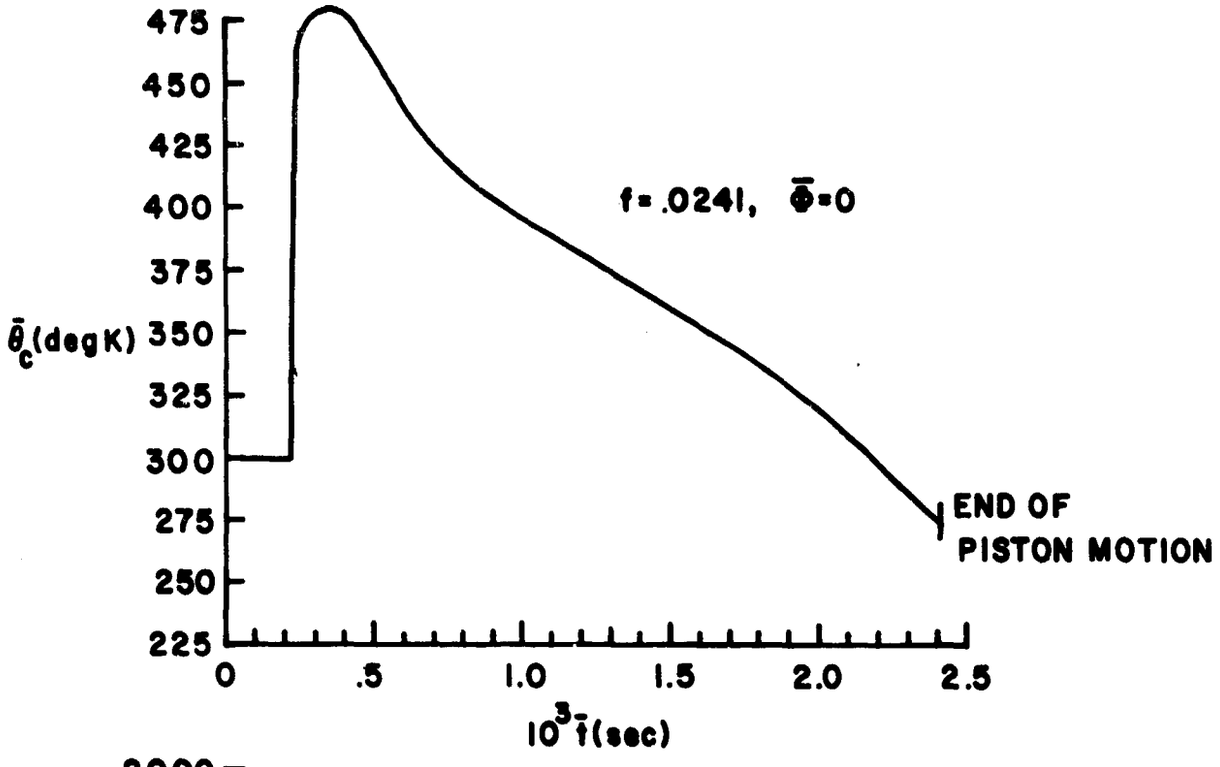

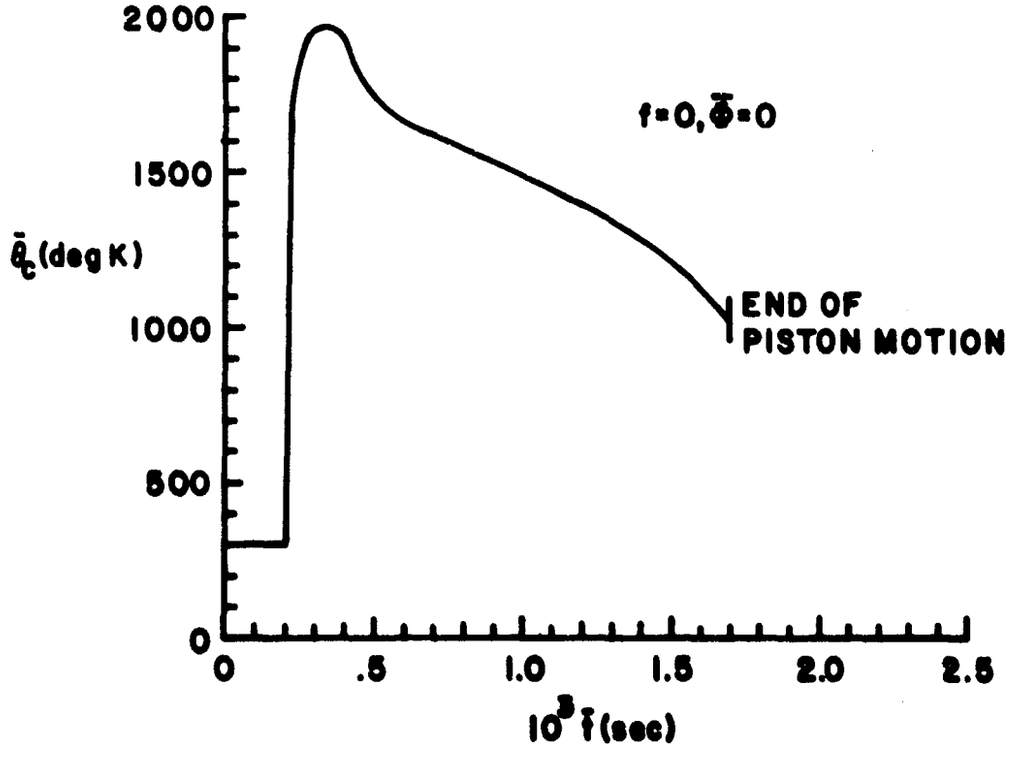

Figure 9. Temperature in Cavity (M-16, Lot #2 Round)

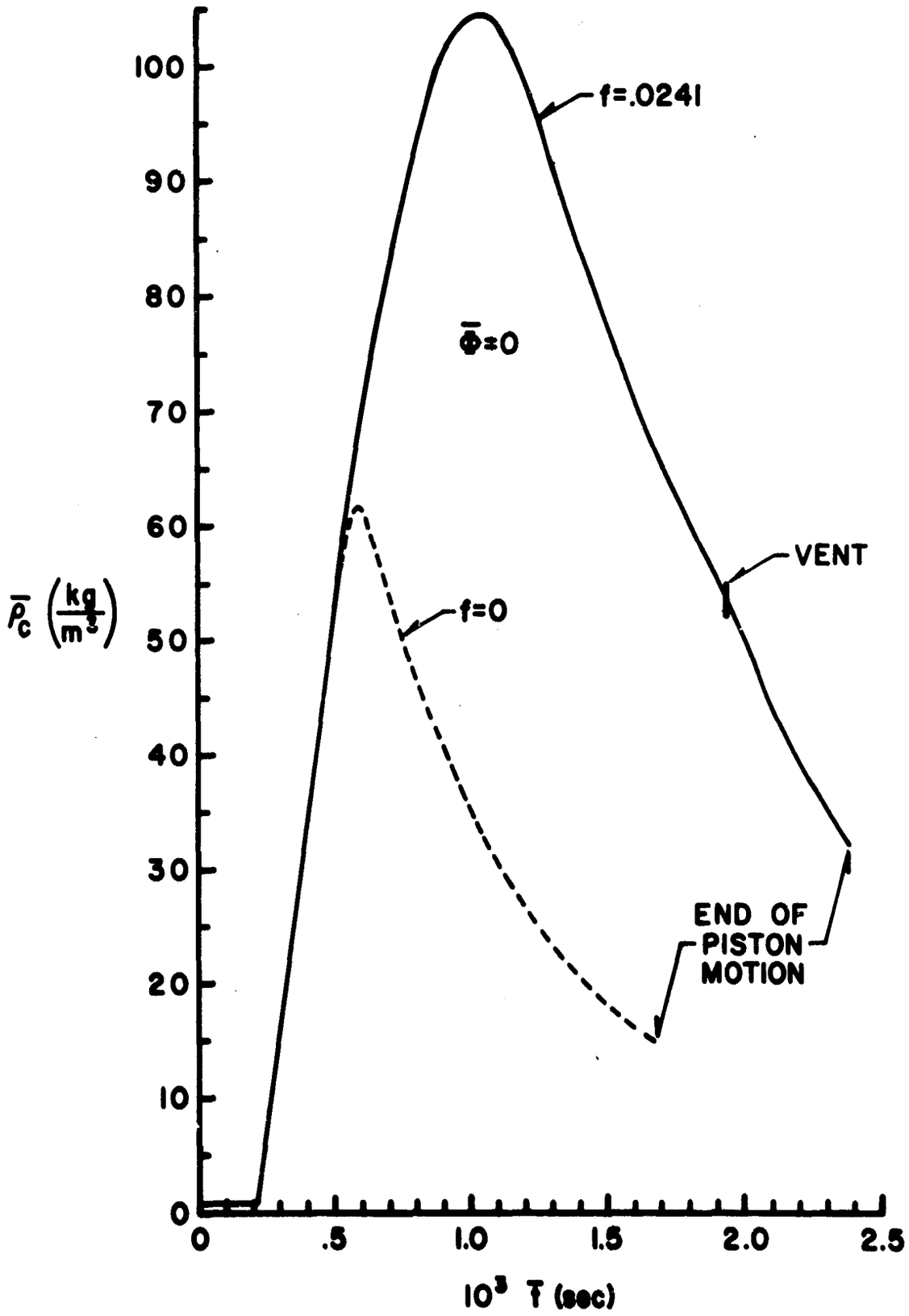

Figure 10. Density in Cavity (M-16, Lot #2 Round)

E. Motion of Piston

The motion of the bolt carrier relative to the bolt is depicted in Figure 11, where relative velocity and bolt carrier displacement are shown. In about 2.4×10^{-3} sec. the piston has moved .0076 m. and attained a relative velocity of 6.3 m/sec.

The velocity, $\bar{v}_{BE}$, of the bolt carrier at time $\bar{t}_E$, when it collides with the bolt, is of interest here, since it is a measure of the momentum applied to the reloading system. Variation of the friction factor f from 0.021 to 0.027 produces less than three percent change from the $\bar{t}_E$ and $\bar{v}_{BE}$ of Figure 11. The $\bar{v}_{BE}$ for the Lot #1 ammunition round differs by less than six percent from that for the Lot #2 round.

Frictional resistance produces retardation; for the case $\bar{p}_z = 0$, $\lambda = 0.3$ it takes 2.8×10^{-3} sec. for the piston to attain a velocity of 5.0 m/sec.

With friction and heat conduction absent from the duct flow (f = 0) a piston velocity of 8.73 m/sec. is reached in 1.7×10^{-3} sec.

IV. AR-18 GAS SYSTEM

A. Discussion

The AR-18 rifle is basically the same gun as the M-16 rifle. It has the same barrel and location of port as the latter; however, the gas system is constructed differently. A sketch of the AR-18 gas system mechanism is presented in Figure 12 at two instants in its cycle: i) beginning of the piston motion, and ii) uncovering of the vents. The dimensions of the system and the loss coefficients are given in APPENDIX A.

A numerical study of the AR-18 gas system was carried out, using input data employed in the M-16 study because of the basic similarity of the two rifles.

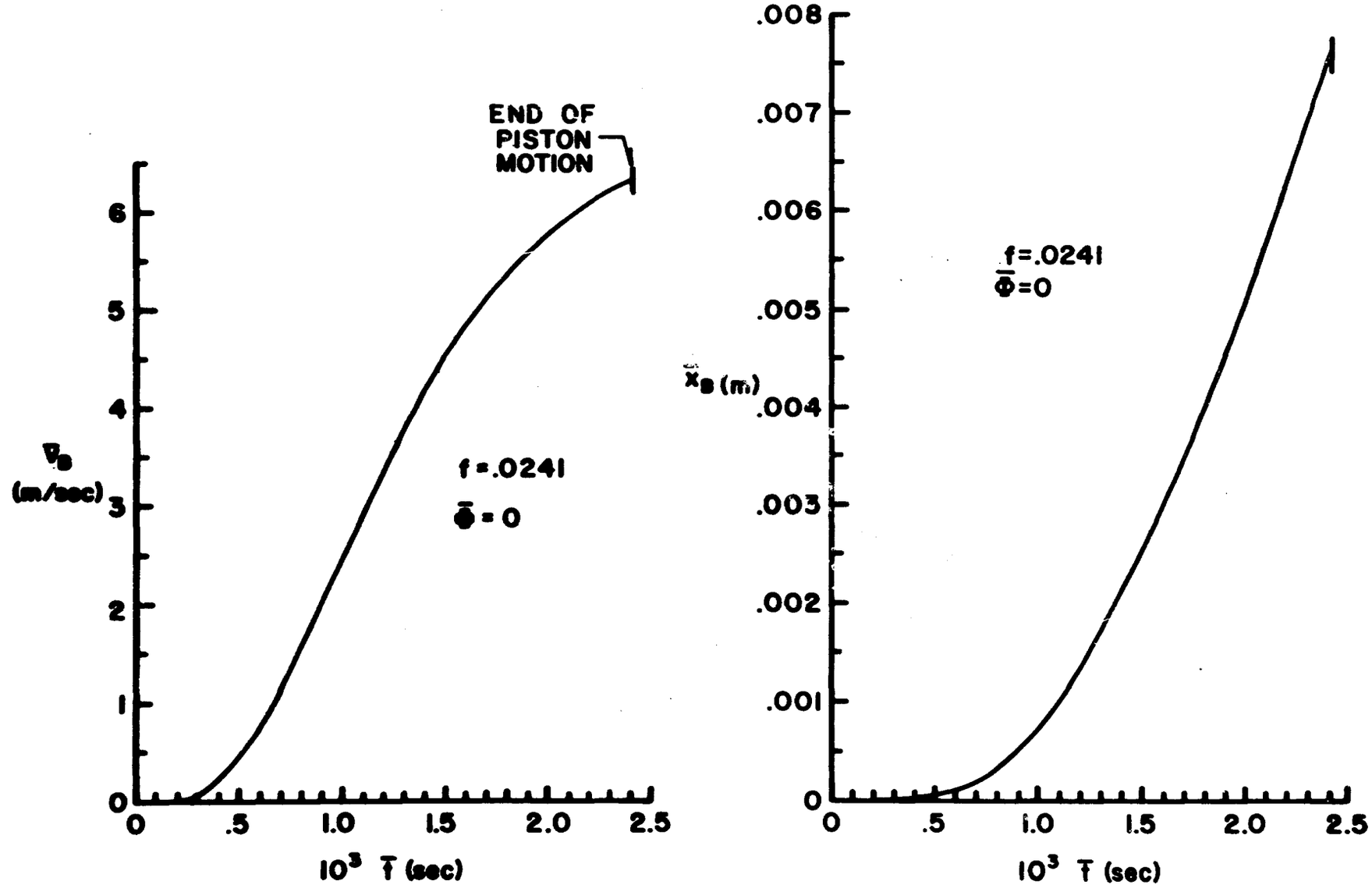

Figure 11. Velocity and Displacement History of Piston (M-16, Lot #2 Round)

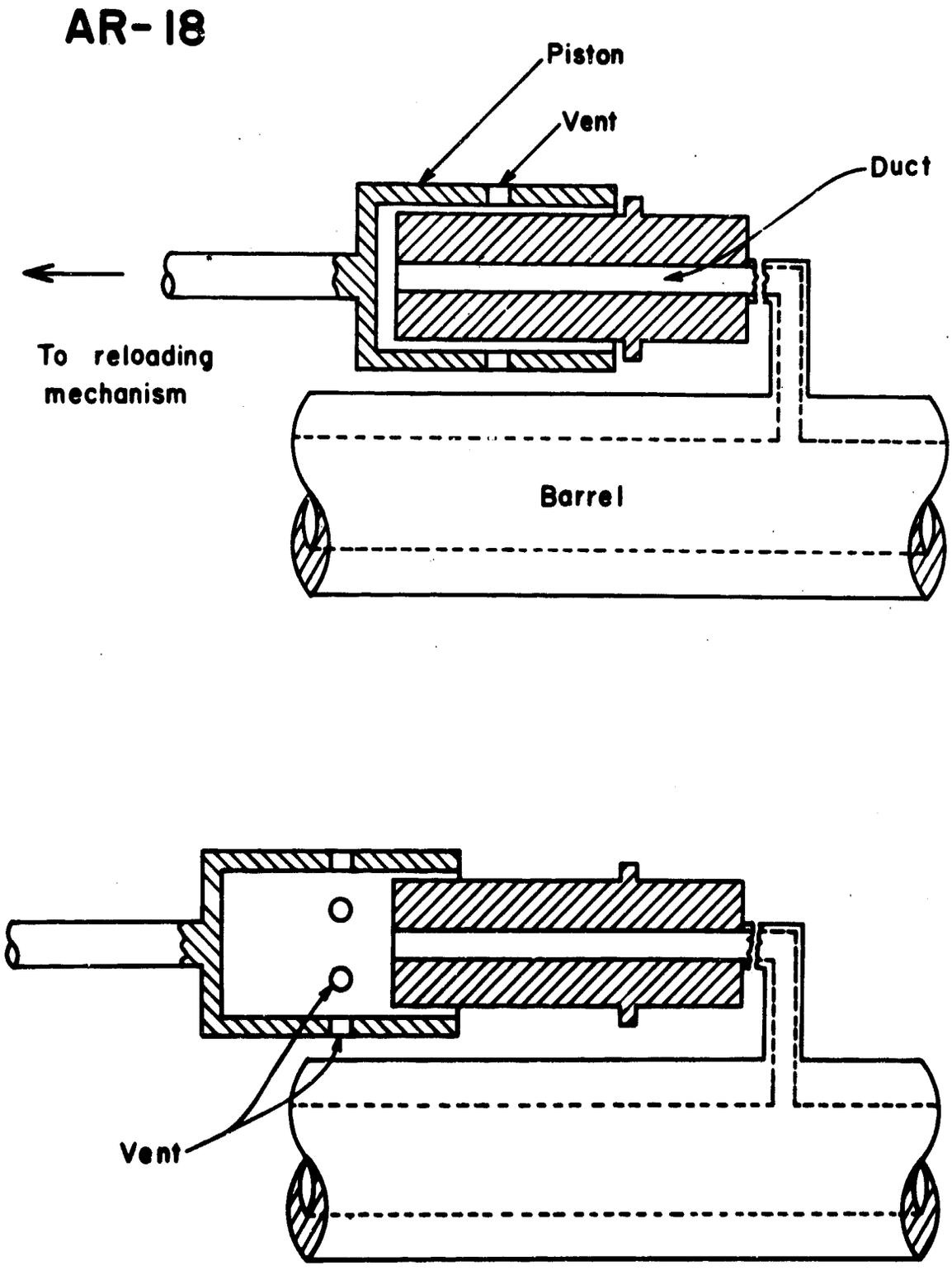

Figure 12. Sketch of AR-18 Rifle Gas System

B. Calculations

The computational results for a round fired in the AR-18 rifle are shown in Figures 13 and 14. Qualitatively the variables behave in the same manner as the corresponding ones in the M-16 rifle. A comparison with measurements of displacement vs time and final velocity of the piston (the only experimental data available) shows good agreement between theory and experiment.

C. Comparison with M-16

While the dynamic and thermodynamic variables are all of the same order of magnitude for the M-16 and AR-18 gas systems, there are quantitative differences due to differences in size of corresponding parts.

Because of the shorter duct length, the delay time (between pressure rise in port and that in cavity) of the AR-18 is about one-fifth of that of the M-16. Venting produces a steeper drop in the thermodynamic quantities in the AR-18, which has a venting area about four times that of the M-16. The peak pressure of the AR-18 is about one and a half times that of the M-16, and the peak temperature is about 100 °K higher in the AR-18.

ACKNOWLEDGEMENT

The author wishes to thank Miss B. Bilsborough for programming and performing the calculations, and Dr. J. H. Spurk for his assistance.

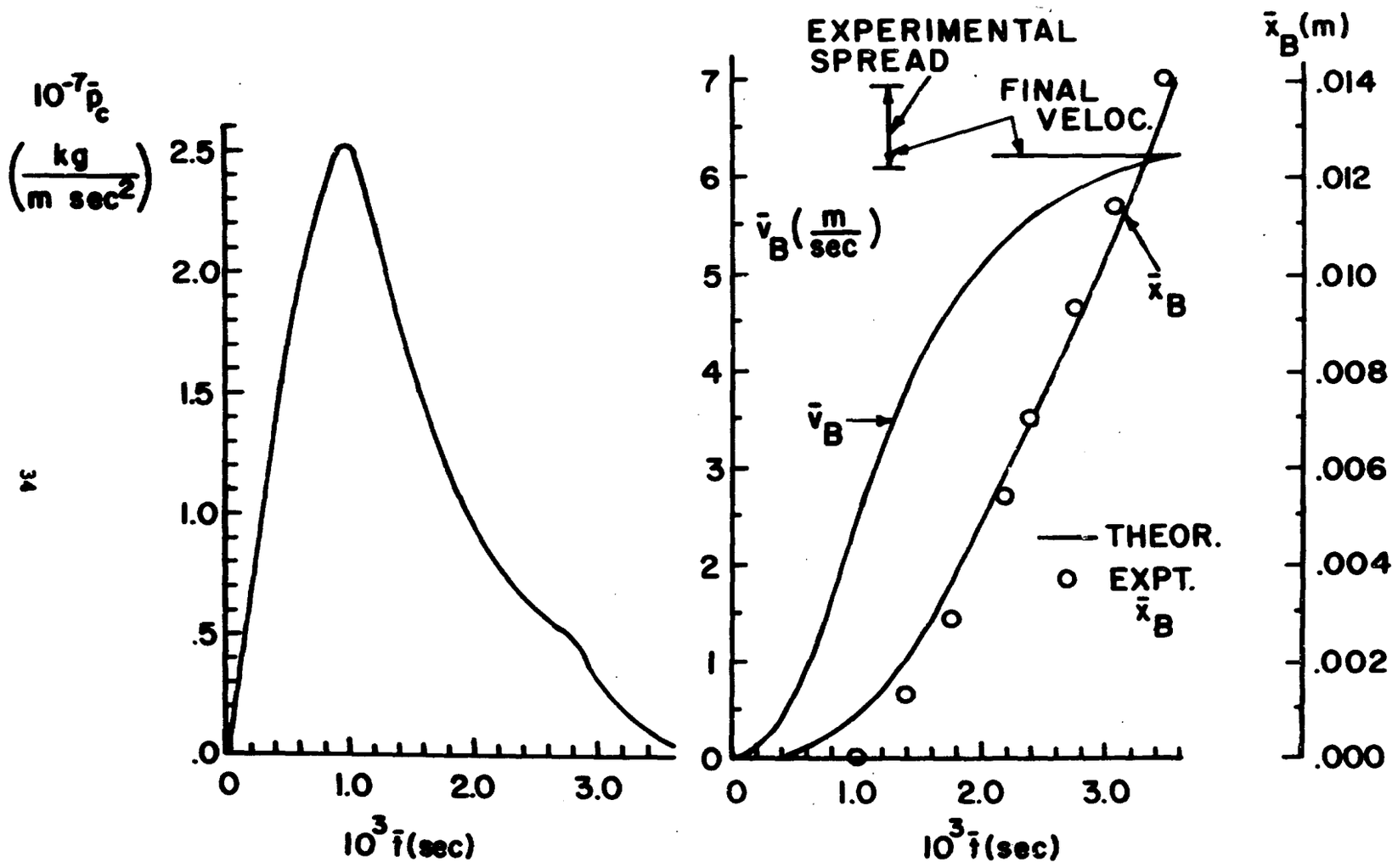

Figure 13. Pressure in Cavity, Piston Velocity and Displacement (AR-18, Lot #2 Round)

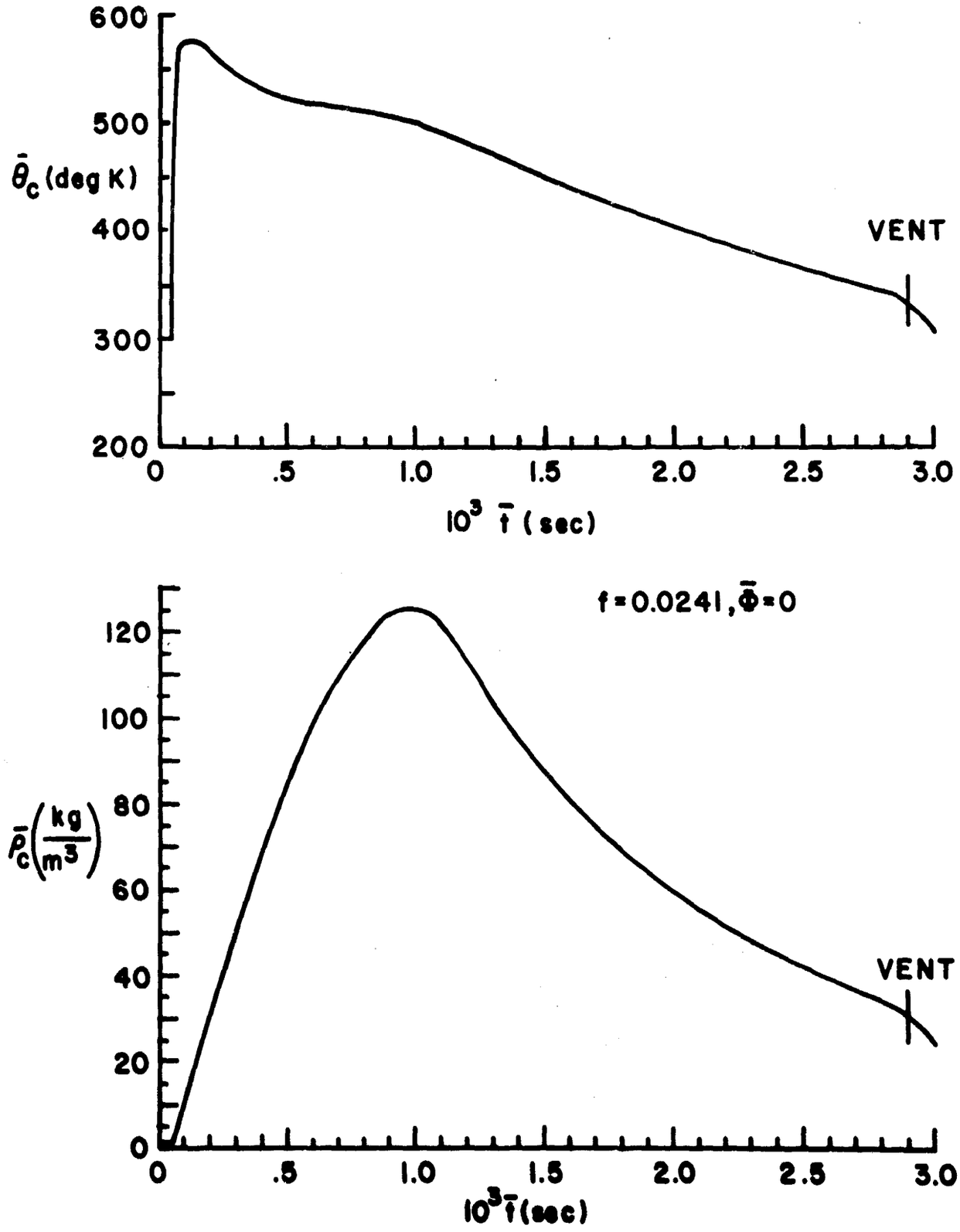

Figure 14. Temperature and Density in Cavity (AR-18, Lot #2 Round)

REFERENCES

1. J. H. Spurk, "The Gas Flow in Gas-operated Weapons," Ballistic Research Laboratories Report No. 1475, February 1970.

2. Crane Technical Paper No. 410, "Flow of Fluids Through Valves, Fittings, and Pipe," Crane Co., Chicago,1969.

APPENDIX A: TABLES OF PARAMETERS*

Table A-I. Properties of Powder Gas**

$\bar{c}_p = 1.74 \times 10^3$ (m/sec)^2/°K

$\bar{c}_v = 1.38 \times 10^3$ (m/sec)^2/°K

$\bar{k} = 0.831 \times 10^{-1}$ (kg m)/(sec^3 °K)

$\bar{R}_{gas} = 0.400 \times 10^3$ (m/sec)^2/°K

$\gamma = 1.26$

$\bar{\gamma} = 1.24$

$\bar{\mu} = 4.80 \times 10^{-5}$ kg/(m sec)

Table A-2. Dimensions of M-16 Gas System

$\bar{A}_c$	$= 1.269 \times 10^{-4}$ m^2	$\bar{M}_B$	$= 0.4366$ kg
$\bar{A}_e$	$= 0.6605 \times 10^{-5}$ m^2	$\bar{r}_v$	$= 0.1442 \times 10^{-2}$ m
$\bar{A}_{min}$	$= 0.4383 \times 10^{-5}$ m^2	$\bar{V}_{ci}$	$= 0.7600 \times 10^{-6}$ m^3
$\bar{A}_p$	$= 0.6605 \times 10^{-5}$ m^2	$\bar{x}_{BE}$	$= 0.7600 \times 10^{-2}$ m
$\bar{A}_v$	$= 0.6533 \times 10^{-5}$ m^2	$\bar{x}_{Bv}$	$= 0.6158 \times 10^{-2}$ m
$\bar{D}$	$= 0.2900 \times 10^{-2}$ m	$(\bar{\epsilon}/\bar{D})$	$= 0.015$
$\bar{l}$	$= 0.3600$ m		

**Values of powder gas properties and dimensions of gas systems supplied by Interior Ballistics Laboratory.*

***Estimates based on the interior ballistics computation of the composition of the powder gas.*

Table A-III. Loss and Flow Coefficients of M-16 Gas System

$\alpha_e = 0.62$	$K_B = 5.04$
$\alpha_p = 0.64$	$K_F = 6.95$
$\alpha_g = 0.62$	$f = 0.0241$

Table A-IV. Dimensions of AR-18 Gas System

$\bar{A}_c = 0.732 \times 10^{-4}\ m^2$	$\bar{M}_B = 0.463\ kg$
$\bar{A}_e = 0.766 \times 10^{-5}\ m^2$	$\bar{r}_v = 0.299 \times 10^{-2}\ m$
$\bar{A}_{min} = 0.195 \times 10^{-5}\ m^2$	$\bar{V}_{ci} = 0.690 \times 10^{-6}\ m^3$
$\bar{A}_p = 0.766 \times 10^{-5}\ m^2$	$\bar{x}_{BE} = 1.57 \times 10^{-2}\ m$
$\bar{A}_v = 2.80 \times 10^{-5}\ m^2$	$\bar{x}_{Bv} = 0.970 \times 10^{-2}\ m$
$\bar{D} = 0.310 \times 10^{-2}\ m$	$(\bar{\epsilon}/\bar{D}) \approx 0.015$
$\bar{\ell} = 0.0660\ m$	

Table A-V. Loss and Flow Coefficients of AR-18 Gas System

$\alpha_e = 0.62$	$K_B = 3.248$
$\alpha_p = 0.64$	$K_F = 1.1815$
$\alpha_g = 0.62$	$f = 0.0525$

APPENDIX B: CONVERSION TABLE

Area: $1\ m^2 = 10.764\ ft^2 = 1550\ in^2$

Density: $1\ kg/m^3 = 0.06243\ lb/ft^3$

Energy: $1\ kg\ (m/sec)^2 = 0.94787 \times 10^{-3}$ BTU

Force: $1\ N = 1\ kg\ m/sec^2 = 0.22482\ lb_{force}$

Length: $1\ m = 3.281\ ft = 39.37$ in.

Mass: $1\ kg = 2.205\ lb_{mass}$

Pressure: $1\ N/m^2 = 1\ kg/(m\ sec^2) = 0.14511 \times 10^{-3}$ psi

Velocity: $1\ m/sec = 3.281\ ft/sec = 39.37$ in/sec

Volume: $1\ m^3 = 35.315\ ft^3 = 61.024 \times 10^3\ in^3$

1 atm. press. $= 0.1013 \times 10^6\ kg/(m\ sec^2) = 14.69$ psi

UNCLASSIFIED

Security Classification

DOCUMENT CONTROL DATA - R & D

(Security classification of title, body of abstract and indexing annotation must be entered when the overall report is classified)

1. ORIGINATING ACTIVITY (Corporate author) Exterior Ballistics Laboratory U.S. Army Ballistic Research Laboratories, ARDC Aberdeen Proving Ground, Maryland 21005	2a. REPORT SECURITY CLASSIFICATION UNCLASSIFIED 2b. GROUP

3. REPORT TITLE

SENSITIVITY STUDY OF RIFLE GAS SYSTEMS.

4. DESCRIPTIVE NOTES (Type of report and inclusive dates)

5. AUTHOR(S) (First name, middle initial, last name)

Nathan Gerber

6. REPORT DATE	7a. TOTAL NO. OF PAGES	7b. NO. OF REFS
January 1971	45	2

8a. CONTRACT OR GRANT NO.	9a. ORIGINATOR'S REPORT NUMBER(S)
b. PROJECT NO. RDT&E No. 1T061102A33D	REPORT NO. 1524
c.	9b. OTHER REPORT NO(S) (Any other numbers that may be assigned this report)
d.	

10. DISTRIBUTION STATEMENT This document is subject to special export controls and each transmittal to foreign governments or foreign nationals may be made only with prior approval of Commanding Officer, U.S. Army Aberdeen Research and Development Center, Aberdeen Proving Ground, Maryland.

11. SUPPLEMENTARY NOTES	12. SPONSORING MILITARY ACTIVITY
	U.S. Army Materiel Command Washington, D. C.

13. ABSTRACT

Results of a sensitivity study of the M-16 rifle gas system are presented; this study is based on a simulation of rifle gas system operation developed in the BRL. The calculations indicate that thermodynamic variables in the bolt carrier cavity are only weakly sensitive to variations in the following parameters: ~~i)~~ pressure and temperature in the gun barrel when the bullet passes the port, ~~ii)~~ friction in the duct flow, and ~~iii)~~ frictional resistance to motion of the bolt carrier. The computational results are sensitive, however, to the chosen origin of time on the oscillogram showing barrel pressure at the port station.

Graphs are presented for a typical round illustrating pressure, temperature, density, and piston motion histories for M-16 and AR-18 rifle gas systems.

DD FORM 1 NOV 68 1473 REPLACES DD FORM 1473, 1 JAN 64, WHICH IS OBSOLETE FOR ARMY USE.

UNCLASSIFIED

Security Classification

14. KEY WORDS	LINK A		LINK B		LINK C	
	ROLE	WT	ROLE	WT	ROLE	WT
Automatic Weapons Rifle Gas System M-16 Rifle Interior Ballistics						